Topology-free design for amplitude death in time-delayed oscillators coupled by a delayed connection

Topology-free design for amplitude death in time-delayed oscillators coupled by a delayed connection

Luan Ba Le, Keiji Konishi,* and Naoyuki Hara
Department of Electrical and Information Systems, Osaka Prefecture University 1–1 Gakuen-cho, Naka-ku, Sakai, Osaka 599-8531, Japan
(Received 19 November 2012; published 9 April 2013)

This paper deals with amplitude death in time-delayed oscillators coupled by a delayed connection with topology uncertainty. A systematic procedure without trial-and-error testing for designing connection parameters is proposed from a robust control theory viewpoint. This procedure has the following two advantages: the designed connection parameters are valid for any network topology and the procedure is valid even for long-delay oscillators. These analytical results are verified by some numerical simulations.

DOI: 10.1103/PhysRevE.87.042908 PACS number(s): 05.45.Xt, 05.45.Gg, 02.30.Yy, 89.75.−k

I. INTRODUCTION

There has been some interest in coupled nonlinear oscillators from the viewpoints of both academia [1,2] and engineering applications [3–6]. A diffusive-connection-induced stabilization of unstable steady states in coupled oscillators, which is often referred to as amplitude death, has been investigated for over two decades [7,8]. Although this phenomenon never occurs in coupled identical oscillators [7,9], a *time-delayed* connection can induce it [10]. Such time-delay-induced death has received considerable attention from analytical [11–23] and experimental [24,25] points of view.

It is generally known that time delays in engineering nonlinear systems induce self-excited oscillations [26], such as in metal cutting processes [27,28] and contact rotating systems [29]. These oscillations have been considered to be harmful in engineering applications. In the case where the self-excited oscillations occur in a number of identical time-delayed nonlinear systems, amplitude death has a great deal of potential to be a candidate phenomenon for suppressing such oscillations [30]. Most previous studies on amplitude death, however, dealt with the stabilization of oscillators without time delay. Recently, amplitude death in a pair of time-delayed oscillators coupled by a delayed connection was analytically investigated, and the analytical results were experimentally confirmed by electronic circuits [32]. Furthermore, Höfener, Sethia, and Gross investigated the stability of large networks consisting of time-delayed oscillators coupled by a delayed connection [33].

For practical situations where death is desirable for engineering applications, it is required to design the connection parameters (i.e., coupling strength and connection delay) by a simple procedure without trial-and-error testing. Previous studies [32,33], however, have focused only on the stability analysis and then did not provide such a procedure. The present paper proposes a systematic procedure for designing the connection parameters. This procedure has the following two advantages: the designed connection parameters are valid for any network topology and the procedure is valid for any long oscillator delay. This procedure is based on the following facts: the stability of time-delayed oscillators coupled by a delayed connection with topology uncertainty can be reduced to that of a time-delay linear system with parameter uncertainty and an uncertain linear system can be analyzed by using robust control theory [34,35]. These analytical results are verified by some numerical simulations.

II. DELAY-COUPLED TIME-DELAYED OSCILLATORS

Consider a network system consisting of scalar nonlinear time-delayed oscillators,

$$\dot{x}_n = -\alpha x_n + f(x_{n,\tau}) + u_n, \tag{1}$$

where $x_n \in \mathbb{R}$ and $u_n \in \mathbb{R}$ are the state variable and the coupling signal of oscillator n, respectively. $f : \mathbb{R} \to \mathbb{R}$ denotes a nonlinear function, and $x_{n,\tau} := x_n(t-\tau)$ is the delayed variable with oscillator delay $\tau \geqslant 0$. Here $\alpha > 0$ is a parameter. As illustrated in Fig. 1, each oscillator is coupled by a delayed connection,

$$u_n = k\left\{x_n - \frac{1}{d_n}\left(\sum_{m=1}^{N} c_{nm}x_{m,T}\right)\right\}, \tag{2}$$

where $k \in \mathbb{R}$ is the coupling strength. This is a kind of diffusive connection. $N \geqslant 2$ and $T \geqslant 0$ are the total number of oscillators and the connection delay, respectively. The network topology is governed by c_{nm}: If oscillator n is connected to oscillator m, then $c_{nm} = c_{mn} = 1$, otherwise $c_{nm} = c_{mn} = 0$. The self-delayed signals $x_{n,T} := x_n(t-T)$ are not allowed to be injected, that is $c_{nn} = 0$. The number of oscillators that are connected to oscillator n, denoted as the degree of oscillator n, is written as $d_n = \sum_{m=1}^{N} c_{nm}$. Suppose that there is no isolated oscillator, that is, $d_n > 0$. Each oscillator (1) without coupling (i.e., $k = 0$) has the fixed point

$$x^* : 0 = -\alpha x^* + f(x^*). \tag{3}$$

A steady state of oscillators (1) coupled by a delayed connection (2) is described by

$$[x_1 \cdots x_N]^T = [x^* \cdots x^*]^T. \tag{4}$$

The fixed point x^* is assumed to be unstable throughout this paper. Note that a delayed connection (2) can change the stability of x^* but cannot move its location. It is generally known that a diffusive-connection-induced stabilization of steady state (4) is often referred to as amplitude death. Note that this network system ($N \geqslant 2$) is an extension of the

*http://www.eis.osakafu-u.ac.jp/∼ecs

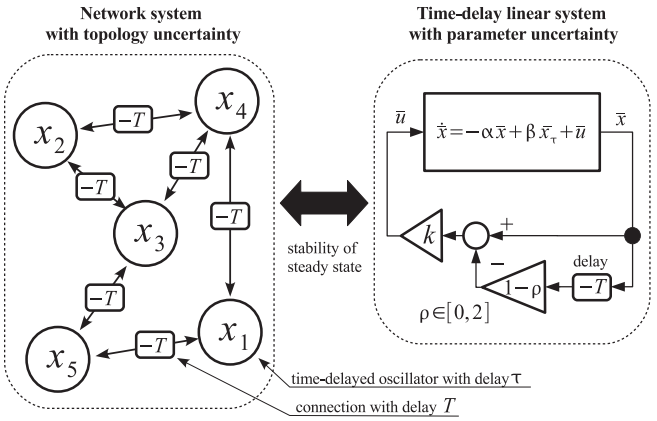

FIG. 1. Illustration of a network system consisting of delayed oscillators (1) coupled by delay connection (2) with topology uncertainty and a time-delay linear system with parameter uncertainty. The stability of steady state (4) in the network is equivalent to that of the linear system.

delay-coupled time-delayed oscillators ($N = 2$) proposed in our previous paper [32].

III. STABILITY ANALYSIS

In order to analyze the linear stability of the steady state, we have to consider the dynamics of the linearized oscillators and connection,

$$\delta\dot{x}_n = -\alpha\delta x_n + \beta\delta x_{n,\tau} + \delta u_n, \tag{5}$$

$$\delta u_n = k\left\{\delta x_n - \frac{1}{d_n}\left(\sum_{m=1}^{N} c_{nm}\delta x_{m,T}\right)\right\}, \tag{6}$$

where $\delta x_n \in \mathbb{R}$ denotes the variation of oscillator n around the fixed point x^*, that is, $\delta x_n := x_n - x^*$. Here $\beta := \{df(x)/dx\}_{x=x^*}$ is the derivative of $f(x)$ at $x = x^*$. The linearized dynamics around the steady state is governed by

$$\delta\dot{\boldsymbol{x}} = (k-\alpha)\delta\boldsymbol{x} + \beta\delta\boldsymbol{x}_\tau - k\boldsymbol{C}\delta\boldsymbol{x}_T, \tag{7}$$

where $\delta\boldsymbol{x} := [\delta x_1 \cdots \delta x_N]^T$. The delayed variations are denoted by $\delta\boldsymbol{x}_\tau := \delta\boldsymbol{x}(t-\tau)$ and $\delta\boldsymbol{x}_T := \delta\boldsymbol{x}(t-T)$. The elements of $\boldsymbol{C}$ are given by $\{\boldsymbol{C}\}_{nm} = c_{nm}/d_n$ for $n \neq m$ and $\{\boldsymbol{C}\}_{nn} = 0$.

The characteristic equation of linear system (7) is described by

$$\det[(s-k+\alpha)\boldsymbol{I}_N - \beta\boldsymbol{I}_N e^{-s\tau} + k\boldsymbol{C}e^{-sT}] = 0, \tag{8}$$

where s is a complex number. This linear system is stable if and only if all the roots s of Eq. (8) are in the open left-half complex plane. Hence, we shall focus on the location of roots s in the complex plane.

Remark that $\boldsymbol{H} := \boldsymbol{I}_N - \boldsymbol{C}$ is similar to a real symmetric matrix $\tilde{\boldsymbol{H}} := \boldsymbol{I}_N - \boldsymbol{D}^{-1/2}\boldsymbol{A}\boldsymbol{D}^{-1/2}$, where $\boldsymbol{D} := \mathrm{diag}\{d_1,\ldots,d_n\}$ and $\boldsymbol{A} := \boldsymbol{D}\boldsymbol{C}$ [36]. Thus, $\boldsymbol{H}$ and $\tilde{\boldsymbol{H}}$ have the same real eigenvalues ρ_q ($q = 1,\ldots,N$). It is generally known that a real symmetric matrix is similar to the diagonal matrix whose diagonal elements are its real eigenvalues. As a consequence, $\boldsymbol{H}$ is similar to the diagonal matrix and then can be diagonalized as

$$\boldsymbol{P}^{-1}\boldsymbol{H}\boldsymbol{P} = \mathrm{diag}(\rho_1,\ldots,\rho_N),$$

where $\boldsymbol{P}$ is a diagonal transformation matrix. It should be noted that the eigenvalues of $\tilde{\boldsymbol{H}}$, which are equivalent to those of $\boldsymbol{H}$, are within the range $\rho_q \in [0,2]$ for any network topology (see Lemma 1.7 in Ref. [37] and Ref. [12] for details):

$$0 = \rho_1 \leqslant \rho_2 \leqslant \cdots \leqslant \rho_N \leqslant 2. \tag{9}$$

This fact allows us to simplify the characteristic equation (8):

$$\begin{aligned} g(s) &= \det[\boldsymbol{P}^{-1}\{(s-k+\alpha-\beta e^{-s\tau})\boldsymbol{I}_N + k\boldsymbol{C}e^{-sT}\}\boldsymbol{P}] \\ &= \det[(s-k+\alpha-\beta e^{-s\tau}+ke^{-sT})\boldsymbol{I}_N \\ &\quad - ke^{-sT}\boldsymbol{P}^{-1}\boldsymbol{H}\boldsymbol{P}] \\ &= \det[(s-k+\alpha-\beta e^{-s\tau}+ke^{-sT})\boldsymbol{I}_N \\ &\quad - ke^{-sT}\mathrm{diag}(\rho_1,\ldots,\rho_N)] \\ &= 0. \end{aligned} \tag{10}$$

As $g(s)$ is a determinant of the diagonal matrix, it can be expressed as a product of the characteristic equations of scalar systems,

$$g(s) := \prod_{q=1}^{N} \bar{g}(s,\rho_q) = 0, \tag{11}$$

where the quasipolynomial $\bar{g}(s,\rho)$ is given by

$$\bar{g}(s,\rho) := s + \alpha - k\{1-(1-\rho)e^{-sT}\} - \beta e^{-s\tau}. \tag{12}$$

It is obvious that the steady state is stable for any network topology if all the roots s of $\bar{g}(s,\rho) = 0$ are in the open left-half complex plane for all $\rho \in [0,2]$. It must be emphasized that $\bar{g}(s,\rho)$ denoted by Eq. (12) is equivalent to the characteristic quasipolynomial of a time-delay linear system with parameter uncertainty (see Fig. 1),

$$\begin{aligned} \dot{\bar{x}} &= -\alpha\bar{x} + \beta\bar{x}_\tau + \bar{u}, \\ \bar{u} &= k\{\bar{x} - (1-\rho)\bar{x}_T\}, \end{aligned} \tag{13}$$

where $\bar{x} \in \mathbb{R}$ is the state variable and $\rho \in [0,2]$ can be treated as an uncertain parameter. We see that the stability of the steady state in the network with oscillators (1) and connection (2) with topology uncertainty is equivalent to that of the linear system (13) with parameter uncertainty. The next section proposes a procedure to design the delayed connection parameters, k and T, such that all of the roots of $\bar{g}(s,\rho) = 0$ are in the open left-half complex plane for all $\rho \in [0,2]$.

IV. DESIGN OF DELAYED CONNECTION

In the previous study [32], it was shown that, if $\alpha < \beta$ holds, amplitude death never occurs at the steady state in a pair of oscillators (i.e., $N = 2$) [38]. Now we extend this property to a network system with oscillators (1) and connection (2).

Lemma 1. Amplitude death never occurs at steady state (4) in a network system consisting of oscillators (1) coupled by connection (2) if $\alpha < \beta$ holds.

Proof. Consider the stability of $\bar{g}(s,0)$. This quasipolynomial at $s = 0$ is $\bar{g}(0,0) = \alpha - \beta$ and, for real positive s, $\bar{g}(s,0) \to +\infty$ as $s \to +\infty$. This implies that, if $\alpha < \beta$ (i.e., $\bar{g}(0,0) < 0$) holds, $\bar{g}(s,0) = 0$ has at least one real positive

root. Since $\rho_1 = 0$ is always held due to Eq. (9), characteristic equation $g(s) = 0$ includes $\bar{g}(s,0) = 0$. Thus, the stability of $\bar{g}(s,0)$ is a necessary condition for that of $g(s) = 0$. As a result, condition $\alpha < \beta$ is a sufficient condition for $g(s)$ to be unstable. ■

The fixed point x^* of oscillators (1) without coupling (i.e., $k = 0$) is stable for any $\tau \geqslant 0$ if $|\beta| < \alpha$ holds (see Sec. 5.2 in Ref. [39]). From this condition and lemma 1, the present paper has to consider oscillators (1) satisfying

$$\beta < -\alpha < 0. \tag{14}$$

This assumption indicates that x^* is unstable and amplitude death may occur at the steady state.

Our main goal is to provide a systematic procedure for designing the coupling strength k and the connection delay T such that the steady state in a network system is stable for any topology $\boldsymbol{C}$ and for any oscillator delay $\tau \geqslant 0$. The eigenvalue $\rho \in [0,2]$, which is the uncertain parameter of $\bar{g}(s,\rho)$, depends on the network topology $\boldsymbol{C}$; therefore, if the family of quasipolynomials,

$$\Omega := \{\bar{g}(s,\rho) \mid \rho \in [0,2]\}, \tag{15}$$

is stable, the stability of the steady state is guaranteed regardless of the network topology. Since all the coefficients of $\bar{g}(s,\rho)$ are affine functions of ρ [see Eq. (12)], the family Ω can be rewritten as a convex combination of the two quasipolynomials, $\bar{g}(s,0)$ and $\bar{g}(s,2)$, in the coefficient space,

$$\Omega := \{(1-\mu)\bar{g}(s,0) + \mu\bar{g}(s,2) \mid \mu \in [0,1]\}, \tag{16}$$

where the one-parameter is given by $\mu := \rho/2$. As a result, $\bar{g}(s,\rho)$ for $\rho \in [0,2]$ denoted by Eq. (15), that is equivalent to the one-parameter family $\bar{g}(s,2\mu)$ for $\mu \in [0,1]$ denoted by Eq. (16), forms a segment with vertices $\bar{g}(s,0)$ and $\bar{g}(s,2)$ in the coefficient space as illustrated in Fig. 2(a). One may conclude that we have to check the stability of the entire segment to guarantee the stability of Ω. This is not true; we can check it by only examining the segment vertices $\bar{g}(s,0)$ and $\bar{g}(s,2)$. In robust control theory [34,35], it is known that Ω is stable if the following two conditions are satisfied:

Condition 1: $\bar{g}(s,0)$ and $\bar{g}(s,2)$ are stable;

Condition 2: $\phi(\omega) := \arg[\bar{g}(j\omega,0)] - \arg[\bar{g}(j\omega,2)] \neq \pm\pi$ for any $\omega \in [0, +\infty)$, where $j^2 = -1$.

Condition 1 provides a stability of the segment vertices $\bar{g}(s,0)$ and $\bar{g}(s,2)$: All the roots of $\bar{g}(s,0) = 0$ and $\bar{g}(s,2) = 0$ are in the open left-half complex plane. These roots never cross the imaginary axis for any $\mu \in (0,1)$, since condition 2 implies that $(1-\mu)\bar{g}(j\omega,0) + \mu\bar{g}(j\omega,2) \neq 0$, as illustrated in Fig. 2(b), holds for any $\omega \in [0, +\infty)$. This is a rough explanation of these conditions: see Ref. [34] and Theorem 4.1.3 in Ref. [35] for its rigorous proof. The following lemmas and corollary provide k and T such that the above two conditions hold.

Lemma 2. $\bar{g}(s,0)$ and $\bar{g}(s,2)$ are stable (i.e., condition 1 holds) if the connection delay $T > 0$ is set to

$$T = \tfrac{1}{2}\tau, \tag{17}$$

and the coupling strength $k < 0$ is chosen from

$$k \in (4\beta - 2\sqrt{2\beta(\beta-\alpha)}, 4\beta + 2\sqrt{2\beta(\beta-\alpha)}). \tag{18}$$

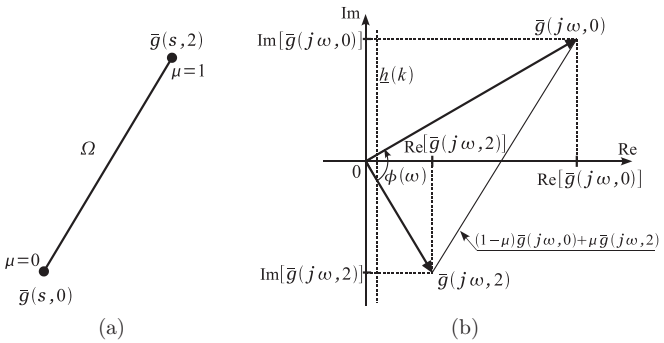

FIG. 2. Sketches of segment Ω and vectors $\bar{g}(j\omega,0)$ and $\bar{g}(j\omega,2)$: (a) Ω with vertices $\bar{g}(s,0)$ and $\bar{g}(s,2)$ in the coefficient space and (b) vectors $\bar{g}(j\omega,0)$ and $\bar{g}(j\omega,2)$ on the complex plane.

Proof. This proof is divided into two steps: step (i) $T = \tau = 0$ and step (ii) $T = \tau/2 \geqslant 0$. Step (i) shall prove that all the roots of $\bar{g}(s,0) = 0$ and $\bar{g}(s,2) = 0$ for $T = \tau = 0$ are in the open left-half complex plane, and step (ii) shall show that these roots with $T = \tau/2 \geqslant 0$ never cross the imaginary axis for any $\tau \in [0, +\infty)$.

For step (i), $T = \tau = 0$ is substituted into $\bar{g}(s,0)$ and $\bar{g}(s,2)$:

$$\bar{g}(s,0) = s + \alpha - \beta, \quad \bar{g}(s,2) = s + \alpha - 2k - \beta.$$

From assumption (14), we notice that all the roots of $\bar{g}(s,0) = 0$ and $\bar{g}(s,2) = 0$ with $T = \tau = 0$ are in the open left-half complex plane for any $k < 0$.

For step (ii), we consider $\bar{g}(j\omega,0) = \mathrm{Re}[\bar{g}(j\omega,0)] + j\mathrm{Im}[\bar{g}(j\omega,0)]$ and $\bar{g}(j\omega,2) = \mathrm{Re}[\bar{g}(j\omega,2)] + j\mathrm{Im}[\bar{g}(j\omega,2)]$. We see that $\bar{g}(j\omega,0) = 0$ is not satisfied for any $\omega \in \mathbb{R}$ [i.e., none of the roots of $\bar{g}(s,0) = 0$ ever cross the imaginary axis] if at least one of $\mathrm{Re}[\bar{g}(j\omega,0)] = 0$ and $\mathrm{Im}[\bar{g}(j\omega,0)] = 0$ does not hold for any $\omega \in \mathbb{R}$. The same holds true for $\bar{g}(j\omega,2) = 0$. Let us show that $\mathrm{Re}[\bar{g}(j\omega,0)] = 0$ and $\mathrm{Re}[\bar{g}(j\omega,2)] = 0$ with $T = \tau/2 \geqslant 0$ do not hold for any $\omega \in \mathbb{R}$. Here $\mathrm{Re}[\bar{g}(j\omega,0)]$

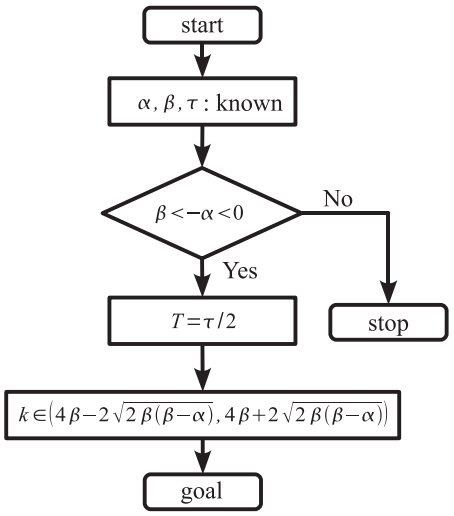

FIG. 3. Flow chart of our systematic procedure for designing k and T. This procedure is based on a sufficient condition for the steady state to be stable.

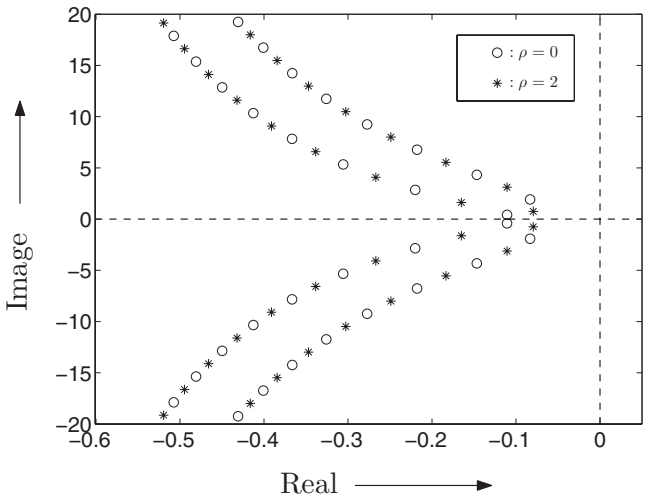

FIG. 4. Roots of $\bar{g}(s,\rho)=0$ ($\rho=0,2$) ($\tau=5, T=2.5, k=-2$).

and $\mathrm{Re}[\bar{g}(j\omega,2)]$ are given by

$$\mathrm{Re}[\bar{g}(j\omega,0)] = \alpha - k + \beta + h_0(\omega\tau),$$
$$\mathrm{Re}[\bar{g}(j\omega,2)] = \alpha - k + \beta + h_2(\omega\tau),$$

where

$$h_0(\omega\tau) := k\cos\frac{\omega\tau}{2} - 2\beta\cos^2\frac{\omega\tau}{2},$$
$$h_2(\omega\tau) := -k\cos\frac{\omega\tau}{2} - 2\beta\cos^2\frac{\omega\tau}{2}.$$

From a simple algebraic computation, we notice that these functions satisfy $h_{0,2}(\omega\tau) \geqslant k^2/(8\beta)$. As a result, we obtain $\mathrm{Re}[\bar{g}(j\omega,0)] \geqslant \underline{h}(k) > 0$ and $\mathrm{Re}[\bar{g}(j\omega,2)] \geqslant \underline{h}(k) > 0$ [see Fig. 2(b)], where

$$\underline{h}(k) := \alpha - k + \beta + \frac{k^2}{8\beta}. \tag{19}$$

These inequalities imply that $\mathrm{Re}[\bar{g}(j\omega,0)] = 0$ and $\mathrm{Re}[\bar{g}(j\omega,2)] = 0$ with $T = \tau/2 \geqslant 0$ do not hold for any $\omega \in \mathbb{R}$. Condition (18) presents the range k satisfying $\underline{h}(k) > 0$. ■

This lemma is equivalent to a design procedure for a pair of oscillators (i.e., $N=2$) [40], since $g(s) = \bar{g}(s,\rho_1)\bar{g}(s,\rho_2) = \bar{g}(s,0)\bar{g}(s,2)$.

Corollary 1. $\phi(\omega) \neq \pm\pi$ for any $\omega \in [0,+\infty)$ holds (i.e., condition 2 holds), if the connection delay $T>0$ and the coupling strength $k<0$ are designed in lemma 2.

Proof. $\phi(\omega) \neq \pm\pi$ suggests that the two vectors $\bar{g}(j\omega,0)$ and $\bar{g}(j\omega,2)$ on the complex plane [see Fig. 2(b)] never have the opposite direction for any $\omega \in [0,+\infty)$. This is obviously true if the real parts of the two vectors are positive,

$$\mathrm{Re}[\bar{g}(j\omega,0)] > 0, \quad \mathrm{Re}[\bar{g}(j\omega,2)] > 0, \quad \forall\omega \in [0,+\infty). \tag{20}$$

Inequalities (20) have been already proved in lemma 2. ■

Note that Eq. (17) and range (18) are independent of each other. This independence implies that the designed k is valid for any $\tau > 0$. As a consequence, lemmas 1 and 2 and corollary 1 obtained above lead to the following main result.

Theorem 1. Assume that oscillators (1) satisfy inequality (14). Steady state (4) in oscillators (1) coupled by connection (2) is stable for any network topology $\boldsymbol{C}$ and for any oscillator delay $\tau > 0$, if the connection delay $T > 0$ is set to Eq. (17) and the coupling strength $k < 0$ is chosen from range (18).

Proof. Since it is obvious from lemmas 1 and 2 and corollary 2, the proof is omitted. ■

This theorem provides a systematic procedure to design the coupling strength k and the connection delay T (see Fig. 3): first, oscillator parameters, α, β, and τ, are known; second, if assumption (14) is not satisfied, then we have to abandon this procedure for designing them; third, T is set to Eq. (17) and $k < 0$ is chosen from range (18). It must be emphasized that k and T designed in accordance with our flow chart illustrated in Fig. 3 are valid for any network topology $\boldsymbol{C}$ and for any $\tau \geqslant 0$. Note that it is possible to reach the goal by other design procedures, since this theorem is based on a sufficient condition for the steady state to be stable.

V. NUMERICAL EXAMPLES

This section numerically confirms the analytical results provided in the preceding sections. Consider oscillators (1)

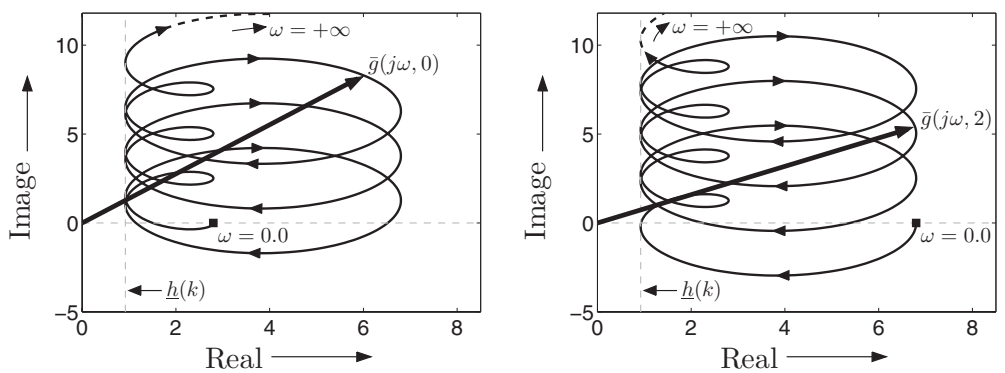

FIG. 5. Vector loci of $\bar{g}(j\omega,0)$ and $\bar{g}(j\omega,2)$ ($\tau=5, T=2.5, k=-2$): (a) $\bar{g}(j\omega,0)$ and (b) $\bar{g}(j\omega,2)$.

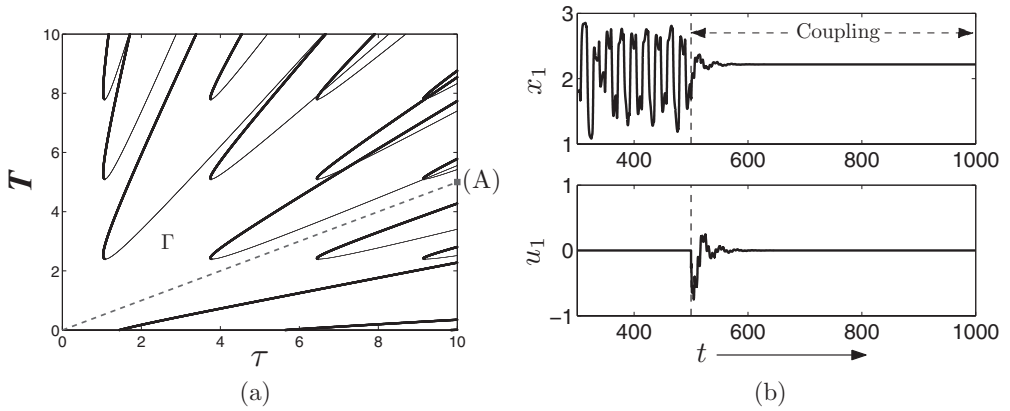

FIG. 6. (Color online) Marginal stability curves and time-series data of the complete network ($N = 200, k = -2$). (a) Marginal stability curves: bold (thin) lines indicate the curves with negative (positive) direction denoted in Eq. (A3). Dashed line indicates $T = \tau/2$ where the sufficient condition for the steady state to be stable always holds. (b) Time-series data of state variable x_1 and coupling signal u_1 at point (A) ($\tau = 10, T = 5$) in (a).

with the parameter $\alpha = 1$ and the nonlinear function,

$$f(x) = \begin{cases} -2.0 & \text{if } x \leqslant -4.25 \\ 0.80x + 1.40 & \text{if } -4.25 < x \leqslant 1.85 \\ -1.80x + 6.21 & \text{if } 1.85 < x \leqslant 3.95 \\ -0.9 & \text{if } x > 3.95 \end{cases}. \quad (21)$$

Each oscillator can be implemented by real electronic circuits [41]. We follow the design procedure illustrated in Fig. 3: first, $\alpha = 1$, $\beta = -1.8$, and $\tau = 5$ are known; second, they satisfy assumption (14) and then go to the next step; third, $T = \tau/2 = 2.5$ and $k = -2 \in (-13.5498, -0.8502)$ are obtained.

Let us confirm that the designed parameters satisfy condition 1 and condition 2 on numerical simulations. Figure 4 shows the roots of $\bar{g}(s,0) = 0$ and $\bar{g}(s,2) = 0$ with the designed parameters. There is no root in the right-half of the complex plane. Thus, we see that $\bar{g}(s,0)$ and $\bar{g}(s,2)$ are stable; that is, condition 1 is satisfied. Figures 5(a) and 5(b) illustrate vector loci of $\bar{g}(j\omega,0)$ and $\bar{g}(j\omega,2)$, respectively, with the designed parameters. It can be seen that each locus is always located on the right side of $\underline{h}(-2) \simeq 0.92 > 0$ denoted by Eq. (19). This result verifies that the two vectors $\bar{g}(j\omega,0)$ and $\bar{g}(j\omega,2)$ never have the opposite direction; that is, condition 2 is satisfied.

Now, we numerically check that the designed parameters are valid for various networks. Note that the parameters were designed on the basis of the sufficient condition, and they must be a subset of the stability region in (τ,T) space. This region consists of the parameter sets (τ,T) where the steady state is stable. The marginal stability curves are obtained by solving $\bar{g}(j\omega,\rho) = 0$ for T and τ. The direction the roots of $\bar{g}(j\omega,\rho) = 0$ cross the imaginary axis depends on the sign of $\mathrm{Re}[ds/dT]_{s=j\omega}$ on the curves. The numerical procedure for estimating the curves and the direction is explained in Appendix. Remark that if the network topology is known in advance, the stability region can be estimated by the numerical procedure. However, the present paper deals with the situation

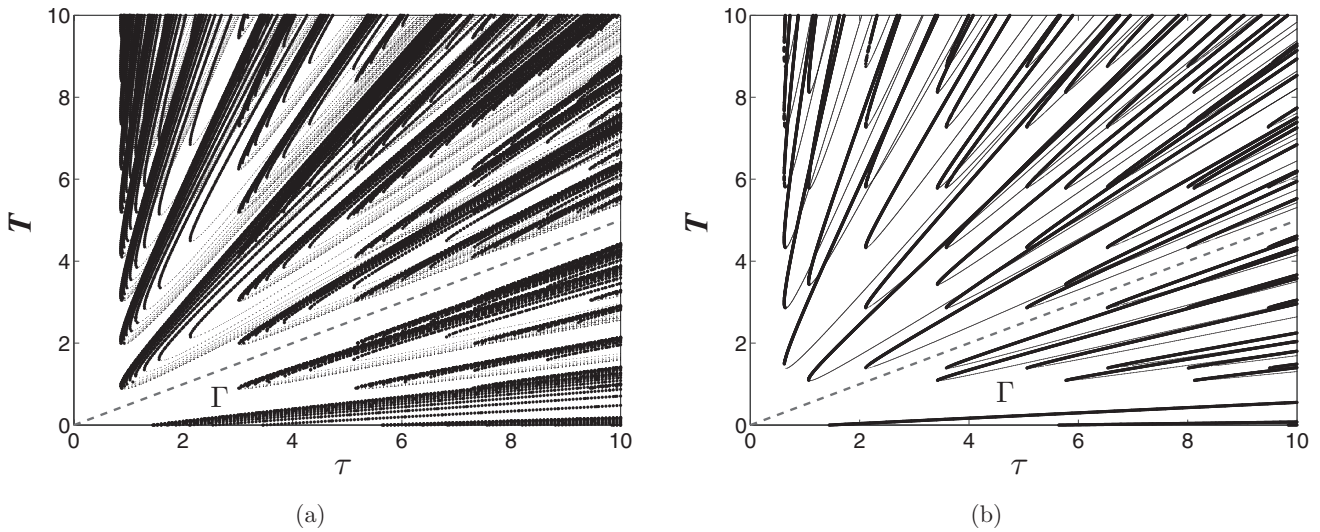

FIG. 7. (Color online) Marginal stability curves of the network system on (a) ring topology ($N = 100, k = -4$) and (b) small-world topology ($N = 50, N_C = 20, k = -10$). Dashed line $T = \tau/2$ indicates the sufficient condition for the steady state to be stable.

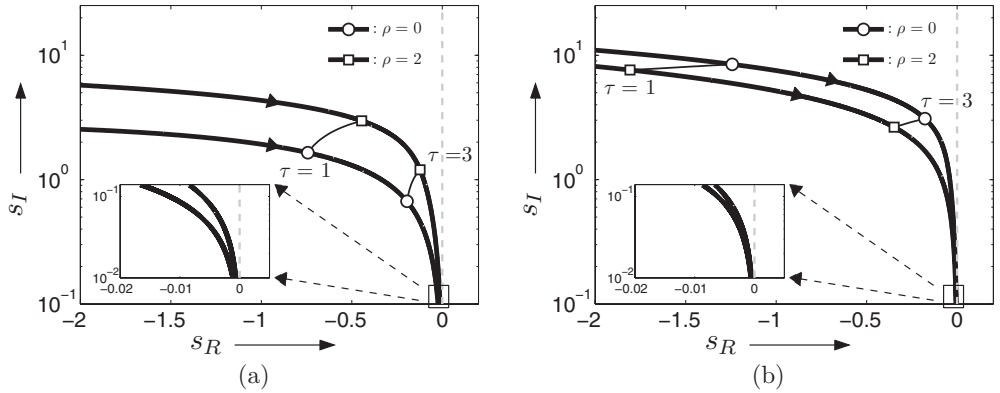

FIG. 8. Root loci of $\bar{g}(s,\rho) = 0$ ($\rho = 0,2$) for $k = -2$: (a) first rightmost root loci, (b) second rightmost root loci.

where the topology is unknown and the region cannot be obtained. In order to check that the designed parameters are valid for various networks, the three typical networks, such as complete networks, ring networks, and small-world networks, are employed.

Consider a complete network (i.e., all-to-all connections) consisting of 200 oscillators ($N = 200$). The eigenvalues of $\boldsymbol{H}$ are $\rho_1 = 0$ and $\rho_{2\text{-}200} = 200/199$. Figure 6(a) illustrates the stability region and the marginal stability curves. The bold (thin) lines indicate the curves with negative (positive) signs of $\mathrm{Re}[ds/dT]_{s=j\omega}$. When T increases and crosses the bold (thin) line upward at a fixed value of τ, we subtract (add) 2 from (to) the number of unstable roots. Since $\bar{g}(s,\rho) = 0$ at the origin (i.e., $\tau = T = 0$) does not have unstable roots, there exist no unstable roots in the region represented by Γ. Furthermore, it must be emphasized that Γ has a long strip including $T = \tau/2$ noted by the dashed line (i.e., this line is a subset of the region Γ). This line never crosses the marginal curves. There is another long strip including $T = \tau$; however, this strip does not exist generally for other networks, as we shall show later. Figure 6(b) shows the time-series data of the first oscillator at point (A) in Fig. 6(a). The state variable x_1 without coupling behaves chaotically until $t = 500$. At $t = 500$ the oscillators are coupled, and then x_1 and the coupling signal u_1 converge on x^* and zero, respectively. It can be seen that, according to our systematic design procedure, the stabilization remains even if the delay times τ and T are extended as long as one wants.

Here we consider networks on a ring topology and a small-world topology with N_C shortcuts [42]. Figures 7(a) and 7(b) illustrate the marginal stability curves for the ring topology ($N = 100, k = -4$) and the small-word topology ($N = 50, N_C = 20, k = -10$), respectively. The eigenvalues of $\boldsymbol{H}$ for the ring topology are $\rho_1 = 0$, $\rho_{2\text{-}99} \in [0.0020, 1.9980]$, and $\rho_{100} = 2$. For the small-world topology, we have $\rho_1 = 0$, $\rho_{2\text{-}50} \in [0.0807, 1.9522]$. The stability regions Γ in Figs. 7(a) and 7(b) contain the long strip including $T = \tau/2$ where the steady state is stable (i.e., this line is a subset of the region Γ). It has to be noted that even though there exist some other long stability strips of (T,τ) in Fig. 6(a) and Fig. 7, they do not always appear for other topologies. Therefore, these strips cannot be used for our topology-free design.

Let us clarify the root distribution of $\bar{g}(s,\rho) = 0$ on the line $T = \tau/2$. Substituting $s = s_R + j s_I$ into $\bar{g}(s,\rho) = 0$ with $T = \tau/2$, we obtain its real and imaginary parts as follows:

$$\begin{aligned}\mathrm{Re}\,[\bar{g}(s,\rho)] &= s_R + \alpha - k + k(1-\rho)e^{-s_R\tau/2}\cos s_I\tau/2 \\ &\quad - \beta e^{-s_R\tau}\cos s_I\tau = 0, \\ \mathrm{Im}\,[\bar{g}(s,\rho)] &= s_I - k(1-\rho)e^{-s_R\tau/2}\sin s_I\tau/2 \\ &\quad + \beta e^{-s_R\tau}\sin s_I\tau = 0. \end{aligned} \tag{22}$$

The roots of $\bar{g}(s,\rho) = 0$ are obtained by solving Eq. (22). Figures 8(a) and 8(b) illustrate the loci of the first and the second right-most roots for $k = -2$, respectively [44]. The bold curves with circles ◯ (squares □) indicate the root loci with $\rho = 0$ ($\rho = 2$) as τ varies from zero to infinity. The thin curves with ◯ and □ ends are the loci at $\tau = 1$ and $\tau = 3$ as ρ varies from zero to 2. For any $\rho \in [0,2]$, the root loci exist between the bold curves with $\rho = 0$ and $\rho = 2$. It can be seen from the insets of Figs. 8(a) and 8(b) that the roots approach asymptotically to the imaginary axis $s_R = 0$ with an increase in τ but never cross the axis. These facts support that there do not exist unstable roots on the line $T = \tau/2$.

VI. CONCLUSION

This paper showed that the stability of a steady state in a network with topology uncertainty is equivalent to the stability of a delayed linear system with parameter uncertainty. A simple sufficient condition for the steady state to be stable is derived on the basis of the robust stability analysis of the linear system. This condition provides us a systematic procedure for designing connection parameters. The procedure has two advantages: the designed parameters can be used for any network topology and the procedure is valid for long-delay oscillators. Our analytical results were numerically verified on complete, ring, and small-world networks.

ACKNOWLEDGMENT

This research was partially supported by JSPS KAKENHI (23560538).

APPENDIX: MARGINAL STABILITY CURVES

The marginal curves of a stability region are obtained by

$$\bar{g}(j\omega,\rho) = j\omega + \alpha - k\{1-(1-\rho)e^{-j\omega T}\} - \beta e^{-j\omega\tau} = 0. \tag{A1}$$

Its real and imaginary parts are described by

$$\begin{aligned} \mathrm{Re}\,[\bar{g}(j\omega,\rho)] &= \alpha - k + k(1-\rho)\cos\omega T - \beta\cos\omega\tau = 0, \\ \mathrm{Im}\,[\bar{g}(j\omega,\rho)] &= \omega - k(1-\rho)\sin\omega T + \beta\sin\omega\tau = 0. \end{aligned} \tag{A2}$$

The marginal stability curves are sketched by using roots T and τ of the above equations. The direction the roots cross the imaginary axis is given by the sign of the real part of $ds/d\tau$ at $s = j\omega$,

$$\mathrm{Re}\left[\frac{ds}{dT}\right]_{s=j\omega} = \mathrm{Re}\left[\frac{j\omega k(1-\rho)e^{-j\omega T}}{1-kT(1-\rho)e^{-j\omega T}+\beta\tau e^{-j\omega\tau}}\right], \tag{A3}$$

where T, τ, and ω satisfy Eq. (A2). With increasing T, a positive (negative) value of Eq. (A3) corresponds to a root crossing the axis from left to right (right to left). The marginal stability curves are estimated by using the following numerical procedure: set a value for τ; solve $\bar{g}(j\omega,\rho) = 0$ for T and ω numerically; check the sign of Eq. (A3); plot (τ, T); change the value of τ; and return to the first step.

[1] A. Pikovsky, M. Rosenblum, and J. Kurths, *Synchronization* (Cambridge University Press, Cambridge, UK, 2001).
[2] S. Boccaletti, V. Latora, Y. Moreno, M. Chavez, and D.-U. Hwang, Phys. Rep. **424**, 175 (2006).
[3] P. Holmes, R. J. Full, D. Koditschek, and J. Guckenheimer, SIAM Rev. **48**, 207 (2006).
[4] A. Ishiguro, M. Shimizu, and T. Kawakatsu, Rob. Auton. Syst. **54**, 641 (2006).
[5] Y.-W. Hong and A. Scaglione, IEEE J. Sel. Areas Comm. **23**, 1085 (2005).
[6] T. Okuda, K. Konishi, and N. Hara, Chaos **21**, 023105 (2011).
[7] D. Aronson, G. Ermentout, and N. Kopell, Physica D **41**, 403 (1990).
[8] Y. Yamaguchi and H. Shimizu, Physica D **11**, 212 (1984).
[9] K. Konishi, Phys. Lett. A **341**, 401 (2005).
[10] D. V. Ramana Reddy, A. Sen, and G. L. Johnston, Phys. Rev. Lett. **80**, 5109 (1998).
[11] D. Reddy, A. Sen, and G. Johnston, Physica D **129**, 15 (1999).
[12] F. M. Atay, J. Differ. Equ. **221**, 190 (2006).
[13] F. M. Atay and O. Karabacak, SIAM J. Appl. Dyn. Syst. **5**, 508 (2006).
[14] C.-Y. Cheng, Phys. Lett. A **374**, 178 (2009).
[15] J. Yang, Phys. Rev. E **76**, 016204 (2007).
[16] K. Konishi, Phys. Rev. E **67**, 017201 (2003).
[17] K. Konishi, H. Kokame, and N. Hara, Phys. Lett. A **374**, 733 (2010).
[18] K. Konishi, H. Kokame, and N. Hara, Phys. Rev. E **81**, 016201 (2010).
[19] R. Dodla, A. Sen, and G. L. Johnston, Phys. Rev. E **69**, 056217 (2004).
[20] M. Mehta and A. Sen, Phys. Lett. A **355**, 202 (2006).
[21] Y. Song, J. Wei, and Y. Yuan, J. Nonlinear Sci. **17**, 145 (2007).
[22] W. Zou and M. Zhan, Phys. Rev. E **80**, 065204 (2009).
[23] G. Saxena, A. Prasad, and R. Ramaswamy, Phys. Rep. (in press).
[24] D. V. Ramana Reddy, A. Sen, and G. L. Johnston, Phys. Rev. Lett. **85**, 3381 (2000).
[25] R. Herrero, M. Figueras, J. Rius, F. Pi, and G. Orriols, Phys. Rev. Lett. **84**, 5312 (2000).
[26] M. Lakshmanan and D. V. Senthilkumar, *Dynamics of Nonlinear Time-Delay Systems* (Springer, Berlin, 2011).
[27] F. C. Moon, *Dynamics and Chaos in Manufacturing Processes* (John Wiley & Sons, New York, 1998).
[28] G. Radons and R. Neugebauer, *Nonlinear Dynamics of Production Systems* (John Wiley & Sons, New York, 2004).
[29] N. Sowa, T. Kondou, H. Mori, and M.-S. Choi, JSME Int. J., Ser. C **49**, 973 (2006).
[30] The relevant concept, the connection control method for suppressing harmful oscillations in flexible structures (e.g., multistory buildings), was proposed in the field of civil engineering [31].
[31] K. Makita, R. E. Christenson, K. Seto, and T. Watanabe, J. Eng. Mech. **133**, 1247 (2007).
[32] K. Konishi, K. Senda, and H. Kokame, Phys. Rev. E **78**, 056216 (2008).
[33] J. M. Höfener, G. C. Sethia, and T. Gross, Europhys. Lett. **95**, 40002 (2011).
[34] V. L. Kharitonov and A. P. Zhabko, IEEE Trans. Autom. Control **39**, 2388 (1994).
[35] H. Y. Hu and Z. H. Wang, *Dynamics of Controlled Mechanical Systems with Delayed Feedback* (Springer, Berlin, 2002).
[36] From $\{\boldsymbol{A}\}_{nm} = \{\boldsymbol{DC}\}_{nm} = c_{nm}$, we see that $\tilde{\boldsymbol{H}}$ is a real symmetric matrix. Further, it is obvious that $\boldsymbol{H}$ is similar to $\tilde{\boldsymbol{H}}$ because $\boldsymbol{H} = \boldsymbol{D}^{-1/2}\tilde{\boldsymbol{H}}\boldsymbol{D}^{1/2}$ holds.
[37] F. R. K. Chung, *Spectral Graph Theory* (American Mathematical Society, Providence, RI, 1997).
[38] This fact implies that the odd number property remains even for amplitude death in a pair of delayed oscillators.
[39] J. K. Hale and S. M. V. Lunel, *Introduction to Functional Differential Equations* (Springer, Berlin, 1993).
[40] L. B. Le, K. Konishi, and N. Hara, in Proceedings of International Scientific Conference on Physics and Control (2011), http://lib.physcon.ru/file?id=2ec7a1700acd.
[41] L. B. Le, K. Konishi, and N. Hara, Nonlinear Dyn. **67**, 1407 (2012).
[42] For the small-world topology [43], every oscillator is coupled on one-dimensional ring-type lattice with periodic boundary and N_C shortcuts, the ends of which are randomly chosen, are added

to the lattice. In particular, the elements c_{nm} are given by the following procedure: $c_{n(n+1)} = c_{(n+1)n} = 1, \forall n \in [1, N-1]$, and $c_{1N} = c_{N1} = 1$; choose N_C pairs of nodes $\{n,m\}$ randomly and connect them as $c_{nm} = c_{mn} = 1$; set the other elements to zero.

[43] C. Moore and M. E. J. Newman, Phys. Rev. E **61**, 5678 (2000).

[44] Since $\bar{g}(s,\rho) = 0$ has an infinite number of roots, an enormous number of loci can be obtained numerically. In order to make clear the loci characteristics, we focus on the first and the second rightmost roots at $\tau = 1$. Figure 8 shows the loci starting from these roots as τ varies. We observed that the other loci have the similar characteristics.